Inverse Volcano: A New Molecule–Surface Interaction Phenomenon

Michelle S. Akerman, Roey Sagi, and Micha Asscher*
Institute of Chemistry, Edmund J. Safra Campus, Givat-Ram The Hebrew University of Jerusalem, Jerusalem 91904, Israel

(Received 17 August 2022; accepted 26 January 2023; published 24 February 2023)

Explosive desorption of guest molecules embedded in amorphous solid water upon its crystallization is known as the "molecular volcano." Here, we describe an abrupt ejection of NH_3 guest molecules from various molecular host films toward a Ru(0001) substrate upon heating, utilizing both temperature programmed contact potential difference and temperature programmed desorption measurements. NH_3 molecules abruptly migrate toward the substrate due to either crystallization or desorption of the host molecules, following an "inverse volcano" process considered a highly probable phenomenon for dipolar guest molecules that strongly interact with the substrate.

DOI: 10.1103/PhysRevLett.130.086203

Contact potential difference (ΔCPD) studies utilizing an *in situ* Kelvin probe can be used as a complement to temperature programmed desorption (ΔP-TPD) measurements within an ultrahigh vacuum (UHV) environment. In contrast to ΔP-TPD studies that track adsorbates as they desorb from a substrate, the noninvasive ΔCPD method is sensitive to the adsorbates' behavior while they are still attached to the substrate. By combining these two methods, an extensive understanding can be obtained about the adsorbate-substrate and adsorbate-adsorbate interactions.

Temperature programmed contact potential difference (TP-ΔCPD) measurements have been employed to study molecular interactions between adsorbates in thin films on a metal substrate [1–7], the self-polarization of thick condensed films [8–10], charging of water films [11–16], and mixing of guest molecules in amorphous solid water (ASW) host films [17]. Previous studies have shown that there is a good, quantitative correlation between the derivative of the TP-ΔCPD $[d(\Delta\mathrm{CPD})/dT]$ and ΔP-TPD spectra, including surface coverage determination [1,6]. Using ΔP-TPD methods, an explosive desorption of N_2 molecules caged in ASW [18] was subsequently coined by Smith *et al.* as the "molecular volcano." In their case, CCl_4 molecules trapped in ASW are abruptly desorbed to the vacuum, as a result of crystallization of the ASW film [19]. This phenomenon has since been discussed extensively for various other guest atoms and molecules trapped exclusively in ASW [18–24]. Recently, it was also reported for methyl chloride molecules caged in amorphous solid ammonia films [10].

In this Letter, we describe a new molecule-surface phenomenon in which guest molecules (NH_3) placed in host films of krypton (Kr), deuterated methyl chloride (CD_3Cl), deuterated methanol (CD_3OD), and water (ASW) are abruptly ejected toward the Ru(0001) substrate. We coin this effect the "inverse volcano" (IV), relating this phenomenon to the molecular volcano. The IV describes the ejection of guest molecules toward the substrate as structural changes occur in the host film prior to or during desorption as the film is heated. NH_3 was chosen as the guest molecule because of its strong interaction with the Ru(0001) substrate, while the host film atoms or molecules were chosen to explore the effect of the diverse host film characteristics on the IV phenomenon.

The ejection of NH_3 molecules to the substrate is studied through TP-ΔCPD measurements, their derivative profiles $[d(\Delta\mathrm{CPD})/dT]$, and ΔP-TPD experiments. The experimental setup and methods have been described elsewhere [16,17] and are briefly summarized here. A single crystal Ru(0001) substrate is held at the center of a UHV chamber with a base pressure of 2×10^{-10} Torr, and is cleaned daily by a 15 min 1000 eV Ne^+ ion sputtering followed by 10 min of annealing at 1450 K. The substrate is exposed to the various gaseous species by backfilling the UHV chamber with the designated gaseous species until the desired film thickness is achieved. The monolayer is determined for each adsorbed species through exposure-dependent ΔP-TPD experiments. Two monolayers (ML) of NH_3 molecules are placed at different locations within host films of Kr, CD_3Cl, CD_3OD, and H_2O 26 ML thick, grown on the Ru(0001) substrate at 35 K (assuming unity sticking probability). The ΔCPD is monitored by a Kelvin probe type S (Besocke Delta-PHI) as adsorption takes place. Once the deposition is complete, the film is heated at a constant rate of 1 K/s while the ΔCPD is recorded in a TP-ΔCPD mode. The IV phenomenon is observed in the derivative mode $[d(\Delta\mathrm{CPD})/dT]$ as a sharp, negative peak [Fig. 1(c)]. A quadrupole mass spectrometer (RGA 200, SRS) is used in separate ΔP-TPD measurements to study the desorption of the prepared films.

In Figs. 1(b) and 1(c), TP-ΔCPD and $d(\Delta\mathrm{CPD})/dT$ spectra for 2 ML of pure NH_3 on Ru(0001) are compared to 2 ML of NH_3 as guest molecules on top of 26 ML thick films of Kr, CD_3Cl, CD_3OD, and under [in direct contact with the Ru(0001) substrate] a 26 ML thick film of H_2O.

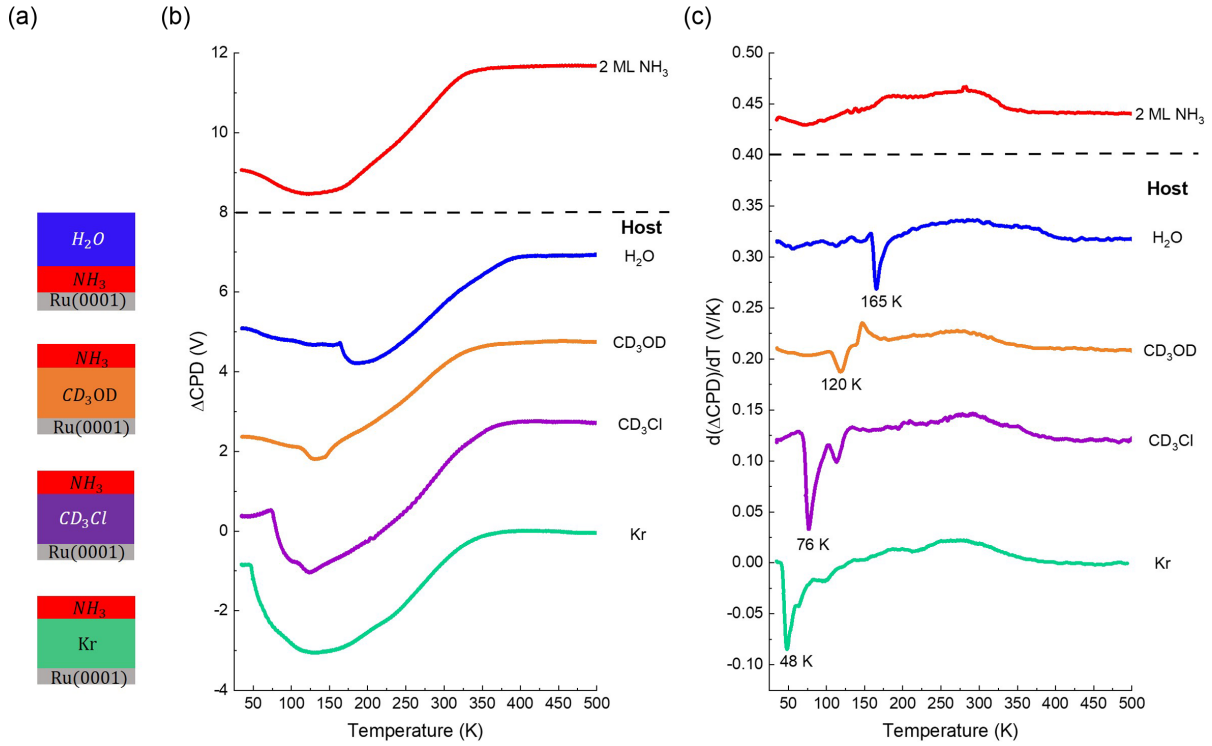

FIG. 1. (a) Illustrations specifying the locations of 2 ML NH_3 in each host film. (b) TP-ΔCPD spectra and (c) their derivative $[d(\Delta\mathrm{CPD})/dT]$ profiles for 2 ML NH_3 on top of 26 ML thick films of Kr (green), CD_3Cl (purple), CD_3OD (orange), and under a 26 ML thick film of H_2O (blue). The films were all adsorbed on a Ru(0001) substrate at 35 K and subsequently heated at a fixed rate of 1 K/s. The negative peak observed in the profiles shown in (c) is referred to as the IV peak. A TP-ΔCPD profile of clean 2 ML NH_3 on Ru(0001) and its derivative profile $d(\Delta\mathrm{CPD})/dT$ are shown in red in both (b) and (c) as a reference. The profiles (except that of Kr) are offset for clarity.

Figure 1(a) contains illustrations to clarify the initial NH_3 position in each host film. The IV peak is observed in all the respective derivative $[d(\Delta\mathrm{CPD})/dT]$ profiles, except in the spectrum of pure NH_3 on Ru(0001). A broad, positive derivative peak is recorded in all the studied films at temperatures where all the host atoms or molecules have already desorbed. This peak is due to the desorbing ammonia molecules following the IV process [see Fig. 1(c)].

Two conditions must be met for the IV phenomenon to occur: First, the guest molecules should interact more strongly with the substrate than the host molecules interact with the substrate, and second, heating the film should induce a change in the molecular composition (guest vs host molecules) at the surface of the substrate. The nature of the host atoms and molecules and their interaction with NH_3 affect the temperature at which the IV occurs. In this study, we looked at the effect of inert (Kr), polar (CD_3Cl), and polar hydrogen bond forming (CD_3OD, H_2O) host atoms and molecules on the IV of the guest NH_3 molecules.

It is possible to track these IV molecules upon their arrival at the substrate. When 2 ML of NH_3 are placed on top of a 26 ML thick Kr film, 96% of the NH_3 molecules migrate to the substrate upon desorption of the Kr multilayer at 48 K [Fig. 1(c) green]. The fraction of NH_3 molecules ejected toward the substrate is estimated by comparing and calibrating the area under the $d(\Delta\mathrm{CPD})/dT$ profile for NH_3@Kr after the IV event to the area obtained this way for 2 ML of clean NH_3 on Ru(0001). In the case of Kr films, there is no crystallization. Therefore, the NH_3 molecules are ejected toward the substrate simultaneously with the desorption of the multilayer. This leads to a drastic negative change in the $d(\Delta\mathrm{CPD})/dT$ spectrum at 48 K. In Fig. 2, a comparison of the $d(\Delta\mathrm{CPD})/dT$ spectrum with the ΔP-TPD profile tracking $m/z = 84$ for Kr shows that the peak temperature for the Kr multilayer desorption at 48 K precisely overlaps the IV peak in the $d(\Delta\mathrm{CPD})/dT$ profile. A redheadlike analysis [25] of the IV spectrum near its peak is used to extract an apparent binding energy of 12.1 ± 0.3 kJ/mol, which is associated with the Kr-NH_3 interaction strength and possibly also reflecting a diffusion barrier of ammonia through the desorbing Kr atoms [26]. In the ΔP-TPD profile, a small peak is observed at 56 K, which is attributed to Kr atom monolayer desorption, which occurs at 58 K [27]. In the $d(\Delta\mathrm{CPD})/dT$ profile, a peak is observed at 62 K, which corresponds with the completion of desorption of the Kr monolayer, as seen by comparing the ΔP-TPD and $d(\Delta\mathrm{CPD})/dT$ profiles (inset Fig. 2). Clean NH_3 molecules eventually desorb from Ru(0001) in

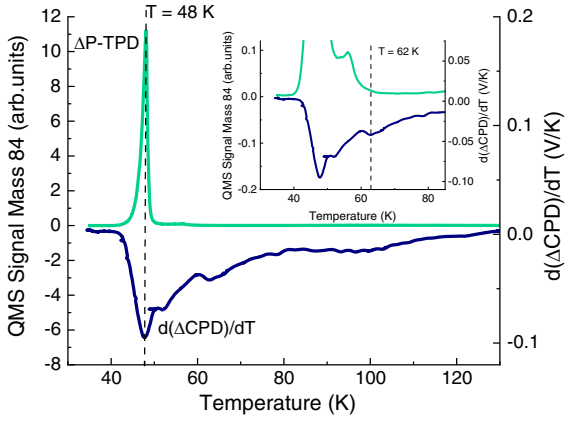

FIG. 2. Comparison between ΔP-TPD (green) and $d(\Delta\mathrm{CPD})/dT$ (navy) profiles for 2 ML of NH_3 adsorbed on top of a 26 ML thick film of Kr at 35 K. Inset: enlargement of the temperature range 35–85 K.

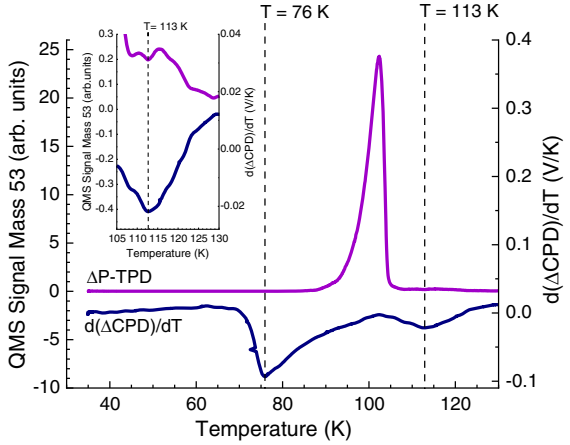

FIG. 3. Comparison between ΔP-TPD (purple) and $d(\Delta\mathrm{CPD})/dT$ (navy) profiles for 2 ML of NH_3 adsorbed on top of a 26 ML thick film of CD_3Cl at 35 K. Inset: enlargement of the temperature range 105–130 K.

a broad, positive $d(\Delta\mathrm{CPD})/dT$ peak extending up to 350 K [10] [see Fig. 1(c), red].

When 2 ML NH_3 are adsorbed on top of a 26 ML thick host film of CD_3Cl, 96% of the NH_3 molecules migrate to the substrate upon crystallization of the CD_3Cl at 76 K, corresponding with an apparent NH_3-CD_3-Cl binding energy (or diffusion barrier) of 19.2 ± 0.3 kJ/mol. In Fig. 3, a comparison between the $d(\Delta\mathrm{CPD})/dT$ and ΔP-TPD ($m/z = 53$) profiles reveals that the IV peak occurs significantly before the desorption of any CD_3Cl is recorded. In contrast to the case of Kr atoms as the host film, it is apparent in the case of CD_3Cl as the host molecules that the signal observed in the $d(\Delta\mathrm{CPD})/dT$ spectrum is related to morphological changes taking place inside the film. In an unpublished study from our group, thick films of CD_3Cl were charged with either Ne^+ ions or low energy electrons and subsequently heated in TP-ΔCPD experiments. The $d(\Delta\mathrm{CPD})/dT$ profiles of both the negatively and positively charged CD_3Cl films show a discharge peak at 75 K. This is an indication that a significant morphological change in the film is taking place, which in this case is likely the crystallization of amorphous CD_3Cl at 75 K. We could not find previously published work regarding this crystallization temperature under UHV conditions. When crystallization of the CD_3Cl film occurs, the NH_3 molecules are ejected toward the Ru(0001) substrate through cracks formed in the film as a result of the crystallization process. At this temperature, desorption of NH_3 and CD_3Cl molecules to the vacuum is not observed (Fig. 3). An additional, smaller peak (negative) in the $d(\Delta\mathrm{CPD})/dT$ profile is observed at 113 K. This may be correlated with the desorption of CD_3Cl molecules that became compressed by the migrating NH_3 molecules on the Ru(0001) substrate or became integrated into the NH_3 monolayer on the substrate. Both CD_3Cl and NH_3 molecules display lateral repulsion between neighboring molecules while adsorbed at monolayer levels on Ru(0001). Both molecules are adsorbed vertically on the Ru(0001) with the hydrogen and methyl groups facing the vacuum and have similar densities in the first adsorbed layer (4.0×10^{14} NH_3 molecules/cm^2 vs 3.6×10^{14} CH_3 Cl molecules/cm^2) [6,28,29]. It is possible that after most of the CD_3Cl molecules have desorbed, some remain bound to the substrate, surrounded by NH_3 molecules that have performed the IV process. A previous study has shown that NH_3 molecules compress and cage CD_3Cl molecules on Ru(0001) [10], similar to the $CD_3Cl@H_2O$ system [30], leading to a lower desorption temperature at the submonolayer. In the $NH_3@CD_3Cl$ case presented here, at the completion of multilayer desorption, the remaining CD_3Cl molecules become incorporated into the NH_3 monolayer. As these CD_3Cl molecules gradually desorb (at 113 K), the NH_3 molecules begin to find their optimal orientation (vertical) on the substrate, resulting in the negative $d(\Delta\mathrm{CPD})/dT$ peak at 113 K, and a continued decrease in the ΔCPD until the NH_3 molecules begin to desorb [see Figs. 3(b) and 3(c)].

Although both CD_3OD and H_2O molecules form hydrogen bonds with NH_3 molecules, the behavior of NH_3 as guest molecules in each of these hosts is different. When 2 ML NH_3 are placed on top of a 26 ML CD_3OD host film, a relatively low intensity IV is observed at 120 K [Fig. 1(b)], around the crystallization temperature of CD_3OD reported in the literature to be 115 K [31]. The extracted apparent binding energy (or diffusion barrier) associated with the NH_3-CD_3OD interaction is 30.5 ± 0.5 kJ/mol. Only 68% of the NH_3 molecules migrate to the substrate. The complicated derivative peak in the case of the CD_3OD host film that includes a positive peak near 146 K is due to the desorption of the methanol multilayer at this temperature [17].

In the case of ASW as the host, in comparison, the IV observed at 165 K is most intense when the 2 ML NH_3

molecules are placed under the 26 ML ASW film, in direct contact with the Ru(0001) substrate and occurs at the multilayer desorption temperature of H_2O [Fig. 1(b)]. The IV is less intense for NH_3 molecules placed on top of an ASW film since most of the NH_3 molecules desorb to the vacuum before the crystallization temperature of ASW is reached. When NH_3 molecules are adsorbed directly on the clean Ru(0001) substrate, they are displaced at the substrate by incoming H_2O molecules [17] and remain trapped inside the ASW film until they are attracted down to the substrate upon multilayer desorption of the water molecules at 165 K. The extracted apparent binding energy or diffusion barrier associated with the NH_3-H_2O interaction is 43.1 ± 0.5 kJ/mol. Following the IV event, 84% of the NH_3 molecules are found at the substrate after all the water molecules have desorbed. These disparities can be explained by the differences in hydrogen bonding propensity of NH_3 with H_2O and NH_3 with CD_3OD. Both H_2O and NH_3 form tetrahedral hydrogen bonded structures, with up to four hydrogen bonds in crystalline ices. In contrast, CD_3OD forms only two hydrogen bonds with neighboring molecules [32,33]. This means that NH_3 molecules can more readily incorporate themselves into an H_2O ice than in a CD_3OD ice. Therefore, when the CD_3OD ice crystallizes, the NH_3 guest molecules are less likely to be incorporated into the ice and are ejected from the film through the cracks that form upon crystallization and are pulled toward the Ru(0001) substrate. Although NH_3 is not easily incorporated into CD_3OD hydrogen bonding network, NH_3 and CD_3OD form a strong hydrogen bond, stronger than that of NH_3 and water [34]. This can hinder the NH_3 migration to the substrate and can explain why a relatively small amount (68%) of NH_3 molecules are found at the substrate following the IV event, indicating that the rest of the NH_3 molecules desorb with the CD_3OD multilayer, as revealed by the positive derivative peak $d(\Delta\mathrm{CPD})/dT$ at 146 K shown in Fig. 1(c).

In the case of NH_3@ASW, upon ASW crystallization at 158 K most of the NH_3 molecules are incorporated within the water-ice crystal structure and do not migrate to the substrate until water desorption occurs at 165 K. The somewhat weaker hydrogen bonds and the higher crystallization temperature explain why a larger fraction of the ammonia molecules (compared to methanol as a host) are ejected toward the substrate (84% for the ASW vs 68% in the CD_3OD case). Ammonia molecules that have not undergone the IV process desorb with the H_2O or CD_3OD host molecules.

Several ΔP-TPD studies have been conducted to study the site competition between adsorbates on TiO_2 (110) [35–37] and forsterite [38] substrates. Although these are not metallic substrates, these studies nevertheless show that an adsorbate can be displaced at the substrate by subsequently adsorbed adsorbates that are characterized by stronger binding to the substrate. For acetone-water [35] and acetone-methanol [36] systems, the water or methanol displacement of acetone occurs before multilayer desorption is observed, but the exact temperature of the displacement was not investigated. Similar observations were reported for the CO_2/H_2O system over the same substrates [37,38].

The TP-ΔCPD measurements and their derivative profiles $[d(\Delta\mathrm{CPD})/dT]$ demonstrate the unique capability to observe *in situ* structural changes within an adsorbed film (host molecule), as the temperature is being increased. Through these methods, one may determine the temperature at which a displacement at the substrate occurs by associating the peak of the IV with the displacement process. This is under the condition that the molecule that binds more strongly to the substrate (the displacing one) leads to a stronger change in CPD.

Whether the IV occurs upon crystallization or desorption of the host molecular ice is dependent on the nature and strength of interaction between the guest molecules and the host molecules in the film as well as the intermolecular interaction among the host molecules (atoms). When the host atom is inert (NH_3@Kr) and does not crystallize prior to its desorption, or when the guest molecule is well incorporated into the crystal structure of the host film (NH_3@ASW), the IV is observed upon desorption of the host atoms or molecules. When the guest molecules are weakly interacting with the host molecules (NH_3@CD_3Cl) or have a high energy barrier for incorporation into the crystal structure of the host (NH_3@CD_3OD), the IV is observed upon crystallization of the host film. As in the case of the volcano desorption, the crystallization energy apparently propels the guest species' motion toward the substrate [19]. The IV peak is correlated with apparent binding (or diffusion barrier) energies ranging from 12.1 to 43.1 kJ/mol with the NH_3-Kr interaction being the weakest and the NH_3-H_2O interaction being the strongest. These values are within 4 kJ/mol of the literature values reported for the heat of vaporization of each pure host film [39], suggesting a correlation between the observed apparent binding energies of the guest molecule and the host molecules' interaction among themselves, thereby affecting the temperature at which the guest molecules can undergo the IV process (see Fig. 1). The temperatures at which the IV occurs are therefore 48, 76, 120, and 165 K for NH_3/Kr, NH_3/CD_3Cl, NH_3/CD_3OD, and NH_3/H_2O, respectively. Our extracted binding strength of NH_3 to the Ru(0001) is significantly stronger than the intermolecular attraction energy of NH_3 to any of the host molecules, characterized by 77.3 kJ/mol at a coverage of about 0.2 ML (lateral repulsion leads to a broad desorption peak).

To summarize, we have demonstrated a new molecule–surface interaction phenomenon, IV, in which guest molecules may be abruptly propelled toward the substrate and not just to the vacuum via the molecular volcano process that has been extensively discussed since 1997 [19]. The direction of migration depends primarily on the nature of

the guest molecule–substrate interaction strength vs the host molecules intermolecular interactions. In cases where the guest molecule binds less strongly to the substrate than the host molecule, the IV is not observed, as in the case of the CD_3Cl@ASW system (not shown). The occurrence of the molecular and inverse volcanos can be considered as mutually exclusive. The fraction of the NH_3 guest molecules found at the ruthenium surface following the host molecules' complete desorption is 68%–96% of the initial 2 ML NH_3 for the systems studied here, as determined by ΔCPD methods following calibration against clean ammonia desorption, as detected by the $[d(\Delta\mathrm{CPD})/dT]$ analysis. Fewer NH_3 molecules were ejected toward the substrate via the IV process when the interaction between the guest and host molecules was stronger.

This study was partially supported by Israel Science Foundation (Grant No. 1406/21) and the Einstein Foundation Berlin. The vital technical support provided by the physics workshop staff (Avner and Rowe) and the electronics workshop staff (Eduard, Marcelo, Shaul, and Alex) is gratefully acknowledged.

M. S. A. performed all the experiments and data analysis and wrote the manuscript. R. S. has participated in some of the analysis and is responsible for all the LabView algorithms. M. A. wrote the manuscript and is responsible for the entire study.

The authors declare no conflicts of interest.

*Corresponding author.
micha.asscher@mail.huji.ac.il

[1] H. Pfnür, P. Feulner, and D. Menzel, The influence of adsorbate interactions on kinetics and equilibrium for CO on Ru(001). II. Desorption kinetics and equilibrium, J. Chem. Phys. **79**, 12 (1983).
[2] J. Kołaczkiewicz and E. Bauer, Temperature Dependence of the Work Function of Adsorbate-Covered Metal Surfaces: A New Method for the Study of Two-Dimensional Phase Transitions, Phys. Rev. Lett. **53**, 485 (1984).
[3] P. Feulner and D. Menzel, The adsorption of hydrogen on ruthenium(001): Adsorption states, dipole moments and kinetics of adsorption and desorption, Surf. Sci. **154**, 465 (1985).
[4] K. L. Kostov, H. Rauscher, and D. Menzel, Adsorption of CO on oxygen-covered Ru(001), Surf. Sci. **278**, 62 (1992).
[5] T. Livneh and M. Asscher, Work function study of the adsorption, lateral repulsion, and fragmentation of CH_3Br on Ru(001), J. Phys. Chem. B **101**, 7505 (1997).
[6] T. Livneh, Y. Lilach, and M. Asscher, Dipole–dipole interactions among CH_3Cl molecules on Ru(001): Correlation between work function change and thermal desorption studies, J. Chem. Phys. **111**, 11138 (1999).
[7] T. Livneh and M. Asscher, The adsorption and decomposition of C_2H_4 on Ru(001): A combined TPR and work function change study, J. Phys. Chem. B **104**, 3355 (2000).
[8] I. K. Gavra, A. N. Pilidi, and A. A. Tsekouras, Spontaneous polarization of vapor-deposited 1-butanol films and its dependence on temperature, J. Chem. Phys. **146**, 104701 (2017).
[9] R. Sagi, M. Akerman, S. Ramakrishnan, and M. Asscher, The role of thermal history on spontaneous polarization and phase transitions of amorphous solid water films studied by contact potential difference measurements, J. Chem. Phys. **153**, 144702 (2020).
[10] R. Sagi, M. Akerman, S. Ramakrishnan, and M. Asscher, Spontaneous polarization of thick solid ammonia films, J. Chem. Phys. **153**, 124707 (2020).
[11] A. A. Tsekouras, M. J. Iedema, and J. P. Cowin, Amorphous Water-Ice Relaxations Measured with Soft-Landed Ions, Phys. Rev. Lett. **80**, 5798 (1998).
[12] Y. Horowitz and M. Asscher, Low energy charged particles interacting with amorphous solid water layers, J. Chem. Phys. **136**, 134701 (2012).
[13] J. Shi, M. Famá, B. D. Teolis, and R. A. Baragiola, Ion-induced electrostatic charging of ice at 15–160 K, Phys. Rev. B **85**, 035424 (2012).
[14] S. Shin, Y. Kim, E. Moon, D. H. Lee, H. Kang, and H. Kang, Generation of strong electric fields in an ice film capacitor, J. Chem. Phys. **139**, 074201 (2013).
[15] R. Sagi, M. Akerman, S. Ramakrishnan, and M. Asscher, Temperature effect on transport, charging, and binding of low-energy electrons interacting with amorphous solid water films, J. Phys. Chem. C **122**, 9985 (2018).
[16] M. Akerman, R. Sagi, and M. Asscher, Charging amorphous solid water films by Ne^+ ions characterized by contact potential difference measurements, J. Phys. Chem. C **124**, 23270 (2020).
[17] M. Akerman, R. Sagi, and M. Asscher, Low-temperature mixing of polar hydrogen bond-forming molecules in amorphous solid water, J. Phys. Chem. C **126**, 6825 (2022).
[18] T. Livneh, L. Romm, and M. Asscher, Cage formation of N_2 under H_2O overlayer on Ru(001), Surf. Sci. **351**, 250 (1996).
[19] R. S. Smith, C. Huang, E. K. L. Wong, and B. D. Kay, The Molecular Volcano: Abrupt CCl_4 Desorption Driven by the Crystallization of Amorphous Solid Water, Phys. Rev. Lett. **79**, 909 (1997).
[20] R. A. May, R. S. Smith, and B. D. Kay, The molecular volcano revisited: Determination of crack propagation and distribution during the crystallization of nanoscale amorphous solid water films, J. Phys. Chem. Lett. **3**, 327 (2012).
[21] R. A. May, R. S. Smith, and B. D. Kay, The release of trapped gases from amorphous solid water films. I. "Top-down" crystallization-induced crack propagation probed using the molecular volcano, J. Chem. Phys. **138**, 104501 (2013).
[22] R. Alan May, R. Scott Smith, and B. D. Kay, The release of trapped gases from amorphous solid water films. II. "Bottom-up" induced desorption pathways, J. Chem. Phys. **138**, 104502 (2013).
[23] R. Souda, Hydration of ammonia, methylamine, and methanol in amorphous solid water, Chem. Phys. Lett. **645**, 27 (2016).

[24] R. Souda, Hydration–dehydration of acetonitrile and methanol in amorphous solid water, J. Phys. Chem. C **120**, 934 (2016).

[25] J. T. Yates, *Experimental Innovations in Surface Science: A Guide to Practical Laboratory Methods and Instruments* (Springer-Verlag, New York, 1998).

[26] V. N. Antonov, J. S. Palmer, P. S. Waggoner, A. S. Bhatti, and J. H. Weaver, Nanoparticle diffusion on desorbing solids: The role of elementary excitations in buffer-layer-assisted growth, Phys. Rev. B **70**, 045406 (2004).

[27] H. Schlichting and D. Menzel, Techniques for attainment, control, and calibration of cryogenic temperatures at small single-crystal samples under ultrahigh vacuum, Rev. Sci. Instrum. **64**, 2013 (1993).

[28] T. Livneh and M. Asscher, The chemistry of CH_3Cl and CH_3Br on Ru(001), Langmuir **14**, 1348 (1998).

[29] C. Benndorf and T. E. Madey, Adsorption and orientation of NH_3 on Ru(001), Surf. Sci. **135**, 164 (1983).

[30] Y. Lilach and M. Asscher, Compression and caging of CD_3Cl by H_2O layers on Ru(001), J. Chem. Phys. **117**, 6730 (2002).

[31] J. Matthiesen, R. S. Smith, and B. D. Kay, Using Rare Gas Permeation to Probe Methanol Diffusion near the Glass Transition Temperature, Phys. Rev. Lett. **103**, 245902 (2009).

[32] K. J. Tauer and W. N. Lipscomb, On the crystal structures, residual entropy and dielectric anomaly of methanol, Acta Crystallogr. **5**, 606 (1952).

[33] B. H. Torrie, S.-X. Weng, and B. M. Powell, Structure of the α-phase of solid methanol, Mol. Phys. **67**, 575 (1989).

[34] A. D. Fortes, I. G. Wood, and K. S. Knight, The crystal structure of perdeuterated methanol monoammoniate ($CD_3OD \cdot ND_3$) determined from neutron powder diffraction data at 4.2 and 180 K, J. Appl. Crystallogr. **42**, 1054 (2009).

[35] M. A. Henderson, Acetone and water on TiO_2 (110): Competition for sites, Langmuir **21**, 3443 (2005).

[36] M. Shen and M. A. Henderson, Site competition during coadsorption of acetone with methanol and water on TiO_2 (110), Langmuir **27**, 9430 (2011).

[37] R. S. Smith, Z. Li, L. Chen, Z. Dohnálek, and B. D. Kay, Adsorption, desorption, and displacement kinetics of H_2O and CO_2 on TiO_2 (110), J. Phys. Chem. B **118**, 8054 (2014).

[38] R. S. Smith, Z. Li, Z. Dohnálek, and B. D. Kay, Adsorption, desorption, and displacement kinetics of H_2O and CO_2 on forsterite, Mg_2SiO_4 (011), J. Phys. Chem. C **118**, 29091 (2014).

[39] Molar enthalpy of vaporization at the boiling point and at 25° C in *CRC Handbook of Chemistry and Physics*, 103rd ed., edited by J. R. Rumble (CRC Press/Taylor & Francis, 2022).